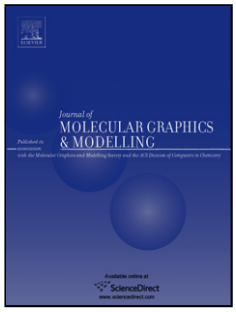

Title: Computational Study of Diketopyrrolopyrrole-based Organic Dyes for Dye Sensitized Solar Cell Applications

Author: Wenjie Fan Dazhi Tan Qijian Zhang Huaxing Wang

PII: S1093-3263(15)00016-9
DOI: http://dx.doi.org/doi:10.1016/j.jmgm.2015.01.006
Reference: JMG 6507

To appear in: *Journal of Molecular Graphics and Modelling*

Received date: 26-7-2014
Revised date: 7-1-2015
Accepted date: 14-1-2015

Please cite this article as: W. Fan, D. Tan, Q. Zhang, H. Wang, Computational Study of Diketopyrrolopyrrole-based Organic Dyes for Dye Sensitized Solar Cell Applications, *Journal of Molecular Graphics and Modelling* (2015), http://dx.doi.org/10.1016/j.jmgm.2015.01.006

Computational Study of Diketopyrrolopyrrole-based Organic Dyes for Dye Sensitized Solar Cell Applications

Wenjie Fan, Dazhi Tan, Qijian Zhang, Huaxing Wang

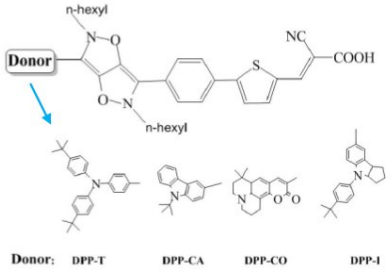

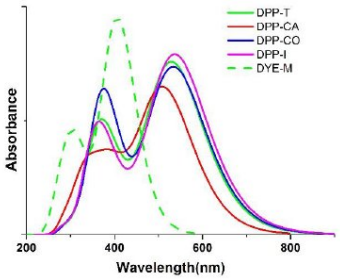

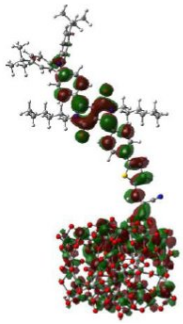

Highlights

> We studied four organic dyes incorporating DPPs moieties. > Electron-deficient DPPs show great effect on spectra and electrochemical properties. > Newly designed DPP-I show desirable energetic and spectroscopic parameters. > We provide theoretical guidance for design of DPP dyes for DSSC optimizations.

Computational Study of Diketopyrrolopyrrole-based Organic Dyes for Dye Sensitized Solar Cell Applications

Wenjie Fan[a,*], Dazhi Tan[b], Qijian Zhang[a], Huaxing Wang[a]

[a] School of Chemical and Environmental Engineering, Liaoning University of Technology, Jinzhou 121001, P.R. China; E-mail: fanwenjie78@gmail.com; Tel.: (+) 0416-4198150; Fax: (+) 0416-4198150

[b] Experimental Center of Chemistry, Faculty of chemical, environmental and biological science and technology, Dalian University of Technology, Dalian 116024, P.R. China

Four diketopyrrolopyrrole (DPP)-based organic dyes utilizing the donor-π-acceptor motif were investigated by density functional theory (DFT) and time-dependent DFT (TDDFT) approaches. The four dyes were composed of different donor groups, i.e. indoline, carbazole, triphenylamine, and coumarin. We investigated the effects of the DPP unit and different donors on the spectra and electrochemical properties of the dyes, respectively. In comparison with the model dye which adopts a phenylene unit as the π-spacer, the DPP dyes all display remarkably enhanced spectral responses in the visible region of the solar spectrum. The key to this increase was the incorporation of electron-deficient DPP moieties to the molecular core, which significantly lowers LUMO levels and therefore reduces the band gap. The dye/$(TiO_2)_{46}$ anatase nanoparticle systems were also simulated to show the electronic structures at the

interface. We studied some key properties including absorption spectra, light-harvesting efficiency, molecular orbital distributions, and injection time of electrons from the excited state of dye to the conduction band of TiO_2. The dye DPP-I with indoline moiety as the electron donor demonstrates desirable energetic, electronic, and spectroscopic parameters for dye sensitized solar cells (DSSCs) applications. Our theoretical study is expected to provide valuable insights into the molecular design of novel DPP-based organic dyes for the optimizations of DSSCs.

Key words: DFT calculations; DSSCs; DPP-based dyes; indoline donor; molecular design

1. Introduction

Dye sensitized solar cells (DSSCs), otherwise known as Grätzel cells after their inventor, are a promising and attractive alternative energy source, with the potential for high efficiency and low-cost power production [1,2]. These cells are composed of a wide band gap semiconductor (typically TiO_2) deposited on a transparent conducting substrate, quasi-monolayer of light harvesting dye molecules, and a redox electrolyte. The dye plays a critical role in DSSCs, since this constituent not only determines the light harvesting properties of the DSSCs, but also mediates the interactions between the redox shuttle and the semiconductor [3, 4]. Until now, the most-promising sensitizers have been Ru complexes, and DSSCs based on Ru^{II}-polypyridyl complexes have an overall solar energy conversion efficiency (η) of more than 11% under simulated AM 1.5 irradiation (100 $mWcm^{-2}$) [5-7]. Metal-free

dyes based on the donor-π -acceptor (D-π-A) motif have also been developed over the past decades owing to their high molar-extinction coefficients, flexible structural modification, and low cost [8, 9]. The record highest η of organic dyes has exceeded 10% [10]. However, organic dyes are still limited from practical applications in DSSCs, due to their relatively narrow absorption bands, unfavorable aggregation on semiconductors, and weaker light stability compared to metal-based dye sensitizers.

Diketopyrrolopyrroles (DPPs) are a class of commercialized and easily synthesized chromophore with exceptional mechanical, photochemical, and thermal stabilities. DPPs have been investigated for optical-electronic applications, such as car-paint pigments [11], small molecule organic photovoltaics [12], solid-state dye lasers [13], organic thin-film transistors [14], and so on. The DPP moiety demonstrates efficient intermolecular charge transfer, which allows for high absorption and benefits the sensitizer to absorb light at infrared wavelength. Furthermore, the electron-withdrawing properties of DPP can assist the electron distribution and greatly stabilize the D-π-A sensitizer. Therefore DPP is a desirable building block for constructing highly efficient sensitizers in DSSCs. Recently, DPP has been considered as a π-conjugated component for applications in DSSCs [15-27]. Jun-Ho Yum and co-workers have reported some synthetically accessible and low-band gap DPP dyes for DSSC applications, and they have completed some structure-property relationship studies for DPP dyes [17, 26]. Recently, they reported the first example of a high-performance blue DSSC: DPP17 yields over 10% power conversion efficiency (PCE) with the $[Co(bpy)_3]^{3+/2+}$ electrolyte at full AM 1.5 G simulated sun light [18].

Qu and Tian have reported a series of metal-free organic dyes that were bridged by a DPP moiety [19-23], and they have compared the phenyl-DPP (PhDPP) and thienyl-DPP (ThDPP) bridge. Recently, Zhang et al synthesized a novel compact dye ICD-1 using a DPP core as a bridge to connect bis(4-tert-butylphenyl)phenylamine and cyanoacetic acid units with the D–π–A configuration. When employed as a sensitizer in DSSCs, ICD-1 gives a high power conversion efficiency of 8.61% under AM 1.5 conditions [27].

For metal-free organic dyes, many types of electron donors have been developed, including coumarin [28], merocyanine [29], indoline [30], polyene [31], triphenylamine [9], et al. Experiments have shown that the donor groups play an important role for DSSCs efficiency. For example, the indoline derivatives can afford strong and intense absorption bands and demonstrate more-powerful electron-donating abilities compared to triphenylamine [30, 32-34].

Being able to accurately predict the electronic and spectroscopic properties of the dyes and the dye/TiO_2 interface, large-scale quantum mechanical calculations would be an extremely powerful and comparably low-cost tool for the interpretation of the experimental data and the beforehand molecular design of novel sensitizers. The conclusions drawn from calculations are valuable guidelines for the synthesis of new efficient dyes. The state-of-the-art computational methodologies density functional theory (DFT) and time-dependent density functional theory (TDDFT) can provide accurate results and reproduce well the structural, electronic, and optical properties of various Ru^{II} complexes [35, 36] and metal-free organic dyes [37-47].

The DPP-based sensitizers have so far exhibited limited applications in DSSCs, which might be due to an incomplete understanding of how to molecularly engineer this promising chromophore into a suitable sensitizer for DSSCs. Theoretically, the effects of the DPP units and different donors on the spectra and electrochemical properties of the DPP-based dyes are still unclear. In this work, DFT/TDDFT investigations were performed to demonstrate how structural modifications affect the energetic, electronic, and spectroscopic properties of the DPP-based sensitizers. Four DPP-based sensitizers utilizing the D-π-A motif were investigated computationally, with DPP core as the π-bridge and cyanoacetic acid as the electron acceptor (shown in Fig.1). As for the choice of the donor group, we considered indoline, carbazole, triphenylamine, and coumarin moieties. A model dye DYE-M with triphenylamine as the donor and phenylene as the π-spacer was also studied for parallel comparison. The dye/$(TiO_2)_{46}$ anatase nanoparticle systems were also simulated to show the electronic properties at the interface. We studied some key properties including absorption spectra, light-harvesting efficiency, molecular orbital distributions, and injection time of electrons from the excited state of dye to the conduction band of TiO_2. Based on the computational investigations, we hope to find more efficient DPP dyes compared with ICD-1.

2. Computational Details

For the isolated organic dyes, all calculations were performed with the Gaussian 09 software [48]. For the ground-state geometric optimization, B3LYP/6-31G(d,p) is selected for the good performance of the geometry optimization of the organic dyes

[38, 44, 45]. Frequency calculations were conducted after geometry optimization to ensure that the dyes are all at the stable point. For the TDDFT calculations of the pure organic dyes, 4 functionals are considered, including one pure density functional PW91 [49], two hybrid functionals B3LYP [50] and PBE0 [51], and CAM-B3LYP functional which is the Handy and co-workers' long-range corrected version of B3LYP using the Coulomb-attenuating method [52]. Solvation effects were investigated performing TDDFT calculations in various solvents with the nonequilibrium version of the C-PCM model [53].

The optimization of dye/$(TiO_2)_{46}$ systems were performed by SIESTA package, employing norm-conserving pseudopotentials (Troullier–Martins nonlocal form) and localized atomic orbitals as basis set [54-56]. The dye/$(TiO_2)_{46}$ structure was considered fully relaxed when the magnitude of forces on the atoms was smaller than 0.04 eV/Å. Standard DFT using the general gradient approximation (GGA) of Perdew, Burke, and Ernzerhof (PBE) [57] and double-ζ plus polarization (DZP) basis set with an equivalent real-space mesh cutoff 250 Ry were used to optimize the geometries. To model the TiO_2 nanoparticle, we used a $(TiO_2)_{46}$ nanocluster, obtained by appropriately 'cutting' an anatase slab exposing the majority (1 0 1) surface [58]. The considered $(TiO_2)_{46}$ nanocluster represents a good trade-off between accuracy and computational convenience and reasonably reproduces the main electronic characteristics of the TiO_2 nanoparticle. The SIESTA optimized dye/$(TiO_2)_{46}$ systems were followed by single point electronic structure analysis, for which we used the B3LYP/6-31G(d) level of computations. The consistency of the results received with

different codes is always kept under control. The GaussSumexe-2.2.5 program was applied for the calculations of densities of states (DOS) partial densities of states (PDOS) [59].

3. Results and Discussion

3.1 Molecular Orbitals

The geometry optimizations show that all the four DPP dyes demonstrate structural similarities, since they possess the same spacer and acceptor moieties. The structural difference results from different donor parts. For the optimized structures, there is coplanarity between the anchoring group and the bridging unit, which is favorable for the electron transfer.

Suitable energy levels and the proper locations of the highest occupied molecular orbital (HOMO) and the lowest unoccupied molecular orbital (LUMO) of the dye sensitizer are required to match the potential of iodine/iodide redox and the conduction band edge level of the TiO_2. The highest few occupied and lowest few unoccupied orbitals are particularly interesting, since they are involved in the electron transitions, in which the photoinduced electron transfers from the excited-state dye to the semiconductor surface. Table 1 lists the HOMO, LUMO energy levels and the HOMO-LUMO gaps of these DPP dyes at B3LYP/6-31G(d,p) level of theory. We found from Table 1 that the orbital levels of DPP dyes are very sensitive to the change in the π-bridge unit and the donor parts.

For DPP-T and DYE-M with the same electron donor and acceptor units, incorporating the electron-deficient DPP moiety into the π bridge conjugation

pathway shifts the LUMO toward the cyanoacrylic acid segment. Replacing benzene unit with the DPP unit in DPP-T effectively lowers the LUMO of DPP-T to -2.86 eV via intramolecular charge transfer compared with that of DYE-M (-2.73 eV). Meanwhile the HOMO energy levels of DPP-T and DYE-M are basically similar. Due to the obvious decreasing LUMO level, the HOMO-LUMO gap of DPP-T is 0.2 eV smaller than that of DYE-M. For the four DPP dyes with the same π-bridge unit and the acceptor parts, the LUMO levels are almost the same, while the donor moieties affect the HOMO levels obviously. The strongly electron donating indoline group in DPP-I effectively raises the HOMO energy level and thus narrows the band gap of the dyes.

The charge-separated states of D-π-A organic dyes are very important in determining the solar cell efficiency. The D-π-A compounds possess photoinduced intramolecular charge-transfer properties which may facilitate rapid electron injection from the dye molecule into the conduction band of the semiconductor. It can be analyzed using spatial orientation models or through the MO contribution of the relevant HOMO and LUMO. To create an efficient charge-separated state, the HOMO must be localized on the donor subunit and the LUMO on the acceptor subunit. Fig. 2 depicts the MO patterns of all dyes considered at the HOMO-1, HOMO, LUMO, and LUMO+1 levels, which might be involved in the photoexcitation processes.

Comparing the DPP-based dyes and the model dye, we found that the presence of electron-deficient DPP units affects on the MO patterns obviously. The incorporation of DPP unit leads to increased localization of the HOMO and LUMO patterns on the

bridging units. For DYE-M, the HOMOs are mainly located at the donor triphenylamine, the LUMOs are mainly centralized on the acceptor and the adjacent thiophene spacer groups, while the bridge benzene parts contributes very little for the HOMO and LUMO. While for the DPP-dyes, take DPP-T as an example, the bridge DPP units contributes a lot for the HOMO.

For the four DPP-based dyes studied, the orbitals show similar distribution features. The HOMO is mainly homogeneously delocalized over the whole donor and DPP units. Since the π bridge and the anchoring units are the same for the four DPP-based dyes, the electron distribution patterns for LUMO orbitals are quite similar: over the DPP core, phenyl unit, thiophene unit, and cyanoacetic acid unit with little contribution from the former. This spatial orientation of HOMO and LUMO of the DPP-dyes is an ideal condition for DSSCs. During light excitation, the electrons will transfer from the donor group through the π bridge to the surface-bound cyanoacrylate, thus facilitating strong coupling of the excited state wave function with the Ti(3d,t2g) orbitals and subsequently favoring the electron injection to the TiO_2 matrix.

3.2 UV/Visible spectrum

For a reasonable computational effort, the state of the art DFT/TDDFT computational methodologies provide reasonable results for metal-free organic dyes [37, 38, 44, 45]. We first examined the effect of the functionals on the excitation energies of the lowest excited state (λ_{max}), and we found that the choice of functionals reveals great effect on the excitation energy. For DPP-T, The calculated lowest excitation energies (oscillator strength, functionals) in CH_2Cl_2 solutions are 717 nm (f

= 0.98, B3LYP), 525 nm (f = 1.56, CAM-B3LYP), 1112 nm (f = 0.55, PW91), and 661 nm (f = 1.17, PBE0). Experimentally, Zhang and co-workers have synthesized DPP-T dye (namely ICD-1 in their work) and it showed absorption maxima at 543 nm in CH_2Cl_2 solutions [27]. Comparing with the experimental absorption, we found that the CAM-B3LYP functional, combined with the 6-311+G(2d,2p) basis set, gives the excitation energies of the lowest excited state at 525 nm in CH_2Cl_2 solvent with a oscillator strength of 1.56, presenting most reliable UV/Vis prediction of ICD-1 dye absorption spectra with a mean absolute deviation of 18 nm. Furthermore, we also found that the absorption spectrum predicted by CAM-B3LYP reproduces well the experimental optical properties. Therefore, on the basis of the agreement with experimental data, CAM-B3LYP is the functional of choice for the UV/Vis spectra calculation.

The simulated electronic absorption spectra of all the DPP dyes dissolved in dichloromethane solvent at CPCM-TDCAM-B3LYP/6-311+G(2d,2p) level of theory are shown in Fig. 3. Table 2 lists the excitation energies of the lowest excited state, oscillator strength *f* and main excitation configuration. Compared with DYE-M, the introduction of DPP moieties reveals strong the effects on the UV/Vis spectra and leads to remarkably 100-130 nm red-shifted absorption bands. In case of DPP-T, the incorporation of a DPP unit displays a remarkable 115 nm red-shifted low-energy excitation than DYE-M.

While for the DPP dyes, our calculations have demonstrated broad absorption spectra with two absorption bands covering a wide range in the visible region: a first

intense peak in the 500–600 nm region and a second peak close to 400 nm, consistent with previous experimental and theoretical studies [18]. The lowest-energy excitation (λ_{max}) for DPP-T, DPP-CO, DPP-I are all around 530 nm, while DPP-CA with coumarin group as the electron donor shows λ_{max} at 509 nm with a much reduced oscillator strength. The red-shift in the charge-transfer (CT) light absorption band in combination with reduced intensity of the CT band in DPP-CA might decrease the light harvesting efficiency and lead to enhanced photocurrent, compared with the other DPP dyes. For DPP-T and DPP-CO, the λ_{max} values are both at 530nm, and DPP-CO shows an enhanced oscillator strength for lowest-energy excitation.

By employing strongly electron donating indoline groups in DPP-I, an 11 nm red-shift in λ_{max} with an enhanced oscillator strength compared to DPP-T was observed. We conjecture that the red-shift CT absorption band in combination with increased intensity of the CT band in DPP-I might increase the light harvesting efficiency and lead to enhanced photocurrent, compared with DPP-T. Experimentally, Yun and coworkers have reported a series of DPP-based dyes [17, 18, 26]. They found that compared with DPP13 bearing triphenylamine as electron donor, employing strongly electron donating indoline groups in DPP14, DPP15, and DPP17 lead to a 10 nm red-shift in the low-energy absorption band and enhanced light harvesting efficiency and photocurrent. Furthermore, they found that DPP17 yields over 10% power conversion efficiency (PCE) with the $[Co(bpy)_3]^{3+/2+}$ electrolyte at full AM 1.5 G simulated sun light, compared to DPP13 with 8.97% PCE [18]. Based on the experiments reported by others [18] and our calculations, we speculate that

incorporating more-powerful donor units into the DPP sensitizer may be a promising approach to further broaden the absorption spectrum.

The light harvesting efficiency (LHE) of the dye should be as high as possible to maximize the photocurrent response [60]. LHE(λ) (LHE at the certain wavelength) can be described by the following equation [[61, 62]

$$LHE(\lambda) = 1 - 10^{-\varepsilon(\lambda)bc} \quad (1)$$

Where ε(λ) is the molar absorption coefficient at certain wavelength, b is the thickness of film, and c is the concentration of dye. It is known that TDDFT is less efficient for the evaluation of transition probabilities than for transition energies. However, it has been reported that the dependence of the experimental extinction coefficient with respect to auxochromic effects was qualitatively reproduced for some organic dyes [38].

To discuss LHE(λ) conveniently, we take the experiment values of b (10 μm) and c (300 mmol L^{-1}), respectively [63-65]. Fig. 4 shows the calculated LHE curves of all the DPP dyes and the model dye. From the LHE curves, we found that at certain wavelength, the corresponding LHE(λ) will be close to one. The LHE of model dye decay rapidly for light wavelengths above 500 nm. While, all the DPP-based dyes show much better light harvesting properties in the visible light region. The LHE data for DPP-I might lead to better photocurrent response than DPP-T.

3.3 Dye/ TiO_2 interface

The precise structure and properties of the electronic excited states of the organic dye/semiconductor interface determine the efficiency of the electron injection, in which the light-excited electrons transfer from the dye into the conduction band of the

semiconductor. Theoretical studies of the dye/semiconductor interface represent an important step towards the optimization of DSSCs. For nanocrystalline TiO_2, it was modeled by a large anatase cluster of 46 units [58]. We performed B3LYP/6-31G(d,p) level single-point calculation on the SIESTA optimized structure. The DOS for the clean $(TiO_2)_{46}$ cluster is shown in Figure S1 in the **supplementary Information.** The bare $(TiO_2)_{46}$ DOS spectra contains reasonably well-developed band structure: a broad substrate valence band and a broad conduction band, separated by a wide band gap. The calculated value for the HOMO-LUMO gap is 4.3 eV, which is in good agreement with previous reports of small TiO_2 clusters [58, 66] but somewhat larger than experimental ~3.4 eV [67] values for anatase TiO_2 nanoparticles. The overestimate of the band gap results from the slight reorganization of the $(TiO_2)_{46}$ geometry compared to crystal structure. Basically, the $(TiO_2)_{46}$ nanoparticle and computational methods used in our study reasonably reproduces the main electronic characteristics of the TiO_2 nanoparticle.

The structure of the dye/$(TiO_2)_{46}$ interacting system is optimized by the SIESTA method, and the SIESTA-optimized dye/$(TiO_2)_{46}$ nanoparticle was followed by single-point electronic structure analysis, using the hybrid B3LYP together with the popular basis set 6-31G(d). The bidentate adsorption mode is energetically favored compared to the monodentate mode for some organic dyes. We therefore simulated the bidentate adsorption mode of the dye DPP-I/$(TiO_2)_{46}$ system with carboxylic oxygen atoms interacting with penta-coordinated surface Ti^{IV} atoms. Our simulations show that the sensitizers studied are adsorbed almost perpendicular to the substrate surface with the formation of two additional Ti-O bonds. After adsorption to the $(TiO_2)_{46}$ cluster, the DPP dyes almost maintain its structure, except for the anchoring group. While for the $(TiO_2)_{46}$ cluster, the formation of two additional Ti–O bonds and the binding of one hydrogen atom to the TiO_2 surface oxygen atom leads to

considerable rearrangements of the surface structures. The average calculated distances between the carboxylic oxygen atoms and the TiO_2 surface (O–Ti bond) are 2.0–2.1 Å.

We also analyzed the frontier molecular orbitals of the DPP-T/$(TiO_2)_{46}$ system. Figure 5 presents the isosurfaces of the HOMO, LUMO, and the interacting orbial (LUMO+41) for the DPP-T/TiO_2 system at a 0.02 au isovalue. We found that the HOMO level of the interacting system corresponds to the HOMO of the free DPP-T, and it is entirely localized on the adsorbate. While the LUMO of the system is just localized on the TiO_2. The interacting orbitals that have non-negligible contributions from the free dye are situated higher up in the conduction band (LUMO+41). This orbital is one of the virtual orbitals that plays a crucial role in the electronic absorption spectrum [68]. The interacting orbital LUMO+41 shows strong mixing of adsorbate π^* and TiO_2 3d orbitals. During light exitation, the electronic coupling and electron transfer takes place between dye's LUMOs and the TiO_2 conduction band. For the other DPP dyes considered in this paper, the MO features after absorption to $(TiO_2)_{46}$ are quite similar to DPP-I.

In order to further understand the adsorption process, we investigated the electronic structures of the sensitizer-nanocrystal systems, by analyzing the total DOS plots of the sensitizer-nanocrystal systems and projected DOS (PDOS) for adsorbed dyes. The features for DOS and PDOS are similar for the four DPP dyes studied, and here only the results for DPP-I are presented in Fig. 6. The sensitizer contributions to the electronic structure, in the region of interest for the photoexcitation processes

involving the sensitizer ground and first excited states, can be demonstrated by focusing on the adsorbate PDOS, which are shown in Fig. 6 with the green line. The DPP-I dye introduces very sharp occupied molecular levels in the band gap, and the new occupied molecular levels become the valence band top of the sensitizer-nanocrystal systems. The HOMO for the DPP dye/TiO_2 system is a DPP dye π-orbital with no coupling to the surface, as also shown in Fig. 5 (a).

3.4 Electron Injections

Although the DOS features for all DPP sensitizer-nanocrystal systems are similar, our calculations predict that the investigated systems differ both in the exact position of the LUMO level and the degree to which the sensitizer LUMO orbital mixes with the conduction band of the substrate TiO_2. The electronic coupling strength governing the photoinduced heterogeneous electron transfer is likely to be determined largely by the interactions between the sensitizer LUMO and the TiO_2 conduction band.

To evaluate the electron injection time (τ, in fs) from the dye to the substrate, a model derived from the Newns-Anderson approach [69] has been considered from the excited state of dye to the conduction band of TiO_2 from the partial densities of states (PDOS) for adsorbed dyes. In this model, by measuring the full width at half maximum of the absorbate LUMO as the energetic broadening (Δ), the electron injection time (τ_{inj}) can be obtained through

$$\tau_{inj}(fs) = 658 / \Delta(meV) \quad (3)$$

$$\Delta = \sum p_i \left| \varepsilon_i - E_{LUMO}(ads) \right| \quad (4)$$

Where p_i is the adsorbate portion of every molecular orbital, εi is orbital energy, and

E_{LUMO}(ads) is the energy of the adsorbate's LUMO.

This model has already been applied to numerous systems including dye/TiO_2 ones [46,70, 71], and it typically provides estimates which are about one-half of the experimental ones. [46] Based on the optimized dye/TiO_2 geometries, we calculated the injection time of electrons from the excited state of dye to the conduction band of TiO_2 for all DPP dyes. The calculated τ_{inj} parameters are 5.98 fs, 5.48 fs, 3.87 fs, and 8.25 fs for DPP-T, DPP-I, DPP-CA, and DPP-CO, respectively. We found that the injection time of electrons from the excited state of DPP dye to the conduction band of TiO_2 all fall in the femtosecond time range with the same order of magnitude, which are all ideal electron-transfer rates for DSSCs applications. Compared to DPP-T, DPP-I dye with the indoline moiety as the donor might accelerate the injection time slightly.

4. Conclusions

DFT/TDDFT investigations were performed to demonstrate how structural modifications affect the energetic, electronic, and spectroscopic properties of the DPP-based sensitizers for DSSCs applications. Four DPP sensitizers utilizing the D-π-A motif were investigated computationally. The four dyes were composed of different donor groups, i.e. indoline, carbazole, triphenylamine, and coumarin. The following conclusions can be received from our calculations: 1) The DPP dyes display remarkably enhanced spectral responses in the visible solar spectrum. The key to this increase was the incorporation of electron-deficient DPP moieties to the molecular core, which significantly lowers LUMO levels and therefore reduces the band gap; 2)

Compared with DPP-T, the red-shift in the charge-transfer light absorption band in combination with increased intensity band in DPP-I might increase the overall light harvesting efficiency and lead to enhanced photocurrent; 3) The DPP sensitizers are adsorbed almost perpendicularly to the $(TiO_2)_{46}$ nanocluster with the formation of two additional Ti-O bonds. The spatial orientation of HOMO and LUMO of dye/$(TiO_2)_{46}$ interface is an ideal condition for DSSCs; 4) The DOS and PDOS calculations show that the DPP-I dye introduces very sharp occupied molecular levels in the band gap, and the new occupied molecular levels become the valence band top of the sensitizer-nanocrystal systems; 5) The injection time of electrons from the excited state of DPP dyes to the conduction band of TiO_2 all falls in the femtosecond time range with the same order of magnitude. Compared with DPP-T, DPP-I dye with the indoline moiety as the donor might accelerate the injection time and lead to higher electron injection efficiency; 6) From the theoretical analysis of absorption spectra, light-harvesting efficiency, molecular orbital distributions, and electron injection time, the dye DPP-I with an indoline moiety as the electron donor demonstrates a balance of the above crucial factors. DPP-I is expected to be a promising dye with desirable energetic and spectroscopic parameters. Our computational studies are expected to shed light on the molecular design of novel DPP dyes for further optimizations of DSSCs.

Acknowledgements

This research was supported by the National Natural Science Foundation of China (grant no. 21103169)

References

[1] B. Oregan, M. Grätzel, A low cost, high-efficiency solar-cell based on dye-sensitized colloidal TiO_2 film, Nature 353 (1991) 737-740.

[2] M. Grätzel, Recent advances in sensitized mesoscopic solar cells, Accounts Chem. Res. 42 (2009) 1788-1798.

[3] P. Gao, Y.J. Kim, J.-H. Yum, T.W. Holcombe, M.K. Nazeeruddin, M. Graetzel, Facile synthesis of a bulky BPTPA donor group suitable for cobalt electrolyte based dye sensitized solar cells, J. Mater. Chem. A 1 (2013) 5535-5544.

[4] S.M. Feldt, E.A. Gibson, E. Gabrielsson, L. Sun, G. Boschloo, A. Hagfeldt, Design of organic dyes and cobalt polypyridine redox mediators for high-efficiency dye-sensitized solar cells, J. Am. Chem. Soc. 132 (2010) 16714-16724.

[5] M. Grätzel, Dye-sensitized solar cells, J. Photochem. Photobiol. C-Photochem. Rev. 4 (2003) 145-153.

[6] F. Gao, Y. Wang, D. Shi, J. Zhang, M. Wang, X. Jing, R. Humphry-Baker, P. Wang, S.M. Zakeeruddin, M. Grätzel, Enhance the optical absorptivity of nanocrystalline TiO_2 film with high molar extinction coefficient ruthenium sensitizers for high performance dye-sensitized solar cells, J. Am. Chem. Soc. 130 (2008) 10720-10728.

[7] F. Sauvage, D. Chen, P. Comte, F. Huang, L. Heiniger, Y.B. Cheng, R.A. Caruso, M. Grätzel, Dye-sensitized solar cells employing a single film of mesoporous TiO_2 beads achieve power conversion efficiencies over 10%. Acs Nano. 4 (2010) 4420-4425.

[8] A. Mishra, M.K.R. Fischer, P. Bauerle, Metal-free organic dyes for dye-sensitized solar cells: from structure, property relationships to design rules, Angew. Chem. Int. Ed. 48 (2009) 2474-2499.

[9] G.L. Zhang, H. Bala, Y.M. Cheng, D. Shi, X.J. Lv, Q.J. Yu, P. Wang, High efficiency and stable dye-sensitized solar cells with an organic chromophore featuring a binary π-conjugated spacer, Chem. Commun. (2009) 2198-2200.

[10] W.D. Zeng, Y.M. Cao, Y. Bai, Y.H. Wang, Y.S. Shi, M. Zhang, F.F. Wang, C.Y. Pan, P. Wang, Efficient dye-sensitized solar cells with an organic photosensitizer featuring orderly conjugated ethylenedioxythiophene and dithienosilole blocks, Chem. Mater. 22 (2010) 1915-1925.

[11] Z.M. Hao, A. Iqbal, Some aspects of organic pigments, Chem. Soc. Rev. 26 (1997) 203-213.

[12] P.M. Beaujuge, J.M.J. Frechet, Molecular design and ordering effects in pi-functional materials for transistor and solar cell applications, J. Am. Chem. Soc. 133 (2011) 20009-20029.

[13] Z. Qiao, Y. B. Xu, S. M. Lin, J. B. Peng, D. R. Cao, Synthesis and characterization of red-emitting diketopyrrolopyrrole-*alt*-phenylenevinylene polymers, Synth. Met. 160 (2010) 1544-1550.

[14] M. Tantiwiwat, N. T. Luu, A. Tamayo, T.-Q. Nguyen, Oligothiophene derivatives functionalized with a diketopyrrolopyrrolo core for solution-processed field effect transistors: effect of alkyl substituents and thermal annealing, J. Phys. Chem. C 112 (2008) 17402-17407.

[15] L. Favereau, J. Warnan, Y. Pellegrin, E. Blart, M. Boujtita, D. Jacquemin, F. Odobel, Diketopyrrolopyrrole derivatives for efficient NiO-based dye-sensitized solar cells, Chem. Commun. 49 (2013) 8018-8020.

[16] T.W. Holcombe, J.-H. Yum, Y. Kim, K. Rakstys, M. Grätzel, Diketopyrrolopyrrole-based sensitizers for dye-sensitized solar cell applications: anchor engineering, J. Mater. Chem. A 1 (2013) 13978-13983.

[17] T.W. Holcombe, J.-H. Yum, J. Yoon, P. Gao, M. Marszalek, D. Di Censo, K. Rakstys, M.K. Nazeeruddin, M. Grätzel, A structural study of DPP-based sensitizers for DSSC applications, Chem. Commun. 48 (2012) 10724-10726.

[18] J.-H. Yum, T.W. Holcombe, Y. Kim, K. Rakstys, T. Moehl, J. Teuscher, J.H. Delcamp, M.K. Nazeeruddin, M. Grätzel, Blue-coloured highly efficient dye-sensitized solar cells by implementing the diketopyrrolopyrrole chromophore, Sci. Rep. 3 (2013) 2446.

[19] S. Qu, C. Qin, A. Islam, J. Hua, H. Chen, H. Tian, L. Han, Tuning the electrical and optical properties of diketopyrrolopyrrole complexes for panchromatic dye-sensitized solar cells, Chem-Asian J. 7 (2012) 2895-2903.

[20] S. Qu, C. Qin, A. Islam, Y. Wu, W. Zhu, J. Hua, H. Tian, L. Han, A novel D-A-pi-A organic sensitizer containing a diketopyrrolopyrrole unit with a branched alkyl chain for highly efficient and stable dye-sensitized solar cells, Chem. Commun. 48 (2012) 6972-6974.

[21] S. Qu, H. Tian, Diketopyrrolopyrrole (DPP)-based materials for organic photovoltaics, Chem. Commun. 48 (2012) 3039-3051.

[22] S. Qu, W. Wu, J. Hua, C. Kong, Y. Long, H. Tian, New diketopyrrolopyrrole (DPP) dyes for efficient dye-sensitized solar cells, J. Phys. Chem. C 114 (2010) 1343-1349.

[23] S.Y. Qu, B. Wang, F.L. Guo, J. Li, W.J. Wu, C. Kong, Y.T. Long, J.L. Hua, New diketo-pyrrolo-pyrrole (DPP) sensitizer containing a furan moiety for efficient and stable dye-sensitized solar cells, Dyes. Pigm. 92 (2012) 1384-1393.

[24] J. Warnan, L. Favereau, F. Meslin, M. Severac, E. Blart, Y. Pellegrin, D. Jacquemin, F. Odobel, Diketopyrrolopyrrole-porphyrin conjugates as broadly absorbing sensitizers for dye-sensitized solar cells, Chemsuschem 5 (2012) 1568-1577.

[25] Y. Wu, W. Zhu, Organic sensitizers from D-pi-A to D-A-pi-A: effect of the internal electron-withdrawing units on molecular absorption, energy levels and photovoltaic performances, Chem. Soc. Rev. 42 (2013) 2039-2058.

[26] J.-H. Yum, T.W. Holcombe, Y. Kim, J. Yoon, K. Rakstys, M.K. Nazeeruddin, M. Grätzel, Towards high-performance DPP-based sensitizers for DSSC applications, Chem. Commun. 48 (2012) 10727-10729.

[27] F. Zhang, K.-J. Jiang, J.-H. Huang, C.-C. Yu, S.-G. Li, M.-G. Chen, L.-M. Yang, Y.-L. Song, A novel compact DPP dye with enhanced light harvesting and charge transfer properties for highly efficient DSSCs, J. Mater. Chem. A 1 (2013) 4858-4863.

[28] Z.S. Wang, Y. Cui, K. Hara, Y. Dan-Oh, C. Kasada, A. Shinpo, A high-light-harvesting-efficiency coumarin dye for stable dye-sensitized solar

cells, Adv. Mater. 19 (2007) 1138-1141.

[29] K. Sayama, K. Hara, N. Mori, M. Satsuki, S. Suga, S. Tsukagoshi, Y. Abe, H. Sugihara, H. Arakawa, Photosensitization of a porous TiO_2 electrode with merocyanine dyes containing a carboxyl group and a long alkyl chain, Chem. Commun. (2000) 1173-1174.

[30] T. Horiuchi, H. Miura, K. Sumioka, S. Uchida, High efficiency of dye-sensitized solar cells based on metal-free indoline dyes, J. Am. Chem. Soc. 126 (2004) 12218-12219.

[31] K. Hara, T. Sato, R. Katoh, A. Furube, T. Yoshihara, M.Murai, M. Kurashige, S. Ito, A. Shinpo, S. Suga, H. Arakawa, Novel conjugated organic dyes for efficient dye-sensitized solar cells, Adv. Funct. Mater. 15 (2005) 246-252.

[32] B. Liu, W. Zhu, Q. Zhang, W. Wu, M. Xu, Z. Ning, Y. Xie, H. Tian, Conveniently synthesized isophoronedyes for high efficiency dye-sensitized solar cells: tuning photovoltaic performance by structural modification of donor group in donor–π–acceptor system, Chem. Commun. (2009) 1766-1768.

[33] W. Zhu, Y. Wu, S. Wang, W. Li, X. Li, J. Chen, Z. Wang, H. Tian, Organic D-A-π-A solar cell sensitizers with improved stability and spectral response, Adv. Funct. Mater. 21 (2011) 756-763.

[34] W. Howie, F. Claeyssens, H. Miura, L. Peter, Characterization of solid-state dye-sensitized solar cells utilizing high absorption coefficient metal-free organic dyes, J. Am. Chem. Soc. 130 (2008) 1367-1375.

[35] L. Salassa, C. Garino, G. Salassa, R. Gobetto, C. Nervi, Mechanism of ligand

photodissociation in photoactivable $[Ru(bpy)(_2)L_2]^{2+}$ complexes: A density functional theory study, J. Am. Chem. Soc. 130 (2008) 9590-9597.

[36] J. F. Guillemoles, V. Barone, L. Joubert, C. Adamo, A theoretical investigation of the ground and excited states of selected Ru and Os polypyridyl molecular dyes, J. Phys. Chem. A, 106 (2002**)** 11354–11360.

[37] M. Pastore, E. Mosconi, F. De Angelis, M. Grätzel, A computational investigation of organic dyes for dye-sensitized solar cells: benchmark, strategies, and open issues, J. Phys. Chem. C 114 (2010) 7205-7212.

[38] J. Preat, C. Michaux, D. Jacquemin, E.A. Perpete, Enhanced efficiency of organic dye-sensitized solar cells: triphenylamine derivatives, J. Phys. Chem. C 113 (2009) 16821-16833.

[39] J. Wang, H. Li, N.-N. Ma, L.-K. Yan, Z.-M. Su, Theoretical studies on organoimido-substituted hexamolybdates dyes for dye-sensitized solar cells (DSSC), Dyes. Pigm. 99 (2013) 440-446.

[40] N. Mohammadi, P.J. Mahon, F. Wang, Toward rational design of organic dye sensitized solar cells (DSSCs): An application to the TA-St-CA dye, J. Mol. Graph. Model. 40 (2013) 64-71.

[41] C.-R. Zhang, L. Liu, Z.-J. Liu, Y.-L. Shen, Y.-T. Sun, Y.-Z. Wu, Y.-H. Chen, L.-H. Yuan, W. Wang, H.-S. Chen, Electronic structures and optical properties of organic dye sensitizer NKX derivatives for solar cells: A theoretical approach, J. Mol. Graph. Model. 38 (2012) 419-429.

[42] J. Zhang, Y.-H. Kan, H.-B. Li, Y. Geng, Y. Wu, Z.-M. Su, How to design proper

pi-spacer order of the D-pi-A dyes for DSSCs? A density functional response, Dyes. Pigm. 95 (2012) 313-321.

[43] C. Zhu, Z. Cao, Unique metal di-porphyrin dyes with excellent photoelectronic properties for solar cells: insight from density functional calculations, Acta. Chim. Sinica. 71 (2013) 1527-1534.

[44] W.J Fan, D.Z Tan, W.Q. Deng, Theoretical investigation of triphenylamine dye/titanium dioxide interface for dye-sensitized solar cells, Phys. Chem. Chem. Phys. 13 (2011) 16159-16167.

[45] W. Fan, D.Z Tan, W.-Q. Deng, Acene-modified triphenylamine dyes for dye-sensitized solar cells: a computational study, Chemphyschem 13 (2012) 2051-2060.

[46] P. Persson, M.J. Lundqvist, R. Ernstorfer, W.A. Goddard, F. Willig, Quantum chemical calculations of the influence of anchor-cum-spacer groups on femtosecond electron transfer times in dye-sensitized semiconductor nanocrystals, J. Chem. Theo. Comp. 2 (2006) 441-451.

[47] W. Zhu, Y. Wu, S. Wang, W. Li, X. Li, J. Chen, Z. Wang, H. Tian, Organic D-A-π-A solar cell sensitizers with improved stability and spectral response, Adv. Funct. Mater. 21 (2011) 756-763.

[48] M.J. Frisch, G.W. Trucks, H.B. Schlegel, G.E. Scuseria, M.A. Robb, J.R. Cheeseman, J.A. Montgomery, T. Vreven, K.N. Kudin, J.C. Burant, J.M. Millam, S.S. Iyengar, J. Tomasi, V. Barone, B. Mennucci, M. Cossi, G. Scalmani, N. Rega, G.A. Petersson, H. Nakatsuji, M. Hada, M. Ehara, K. Toyota, R. Fukuda, J.

Hasegawa, M. Ishida, T. Nakajima, Y. Honda, O. Kitao, H. Nakai, M. Klene, X. Li, J.E. Knox, H.P. Hratchian, J.B. Cross, V. Bakken, C. Adamo, J. Jaramillo, R. Gomperts, R.E. Stratmann, O. Yazyev, A.J. Austin, R. Cammi, C. Pomelli, J.W. Ochterski, P.Y. Ayala, K. Morokuma, G.A. Voth, P. Salvador, J.J. Dannenberg, V.G. Zakrzewski, S. Dapprich, A.D. Daniels, M.C. Strain, O. Farkas, D.K. Malick, A.D. Rabuck, K. Raghavachari, J.B. Foresman, J.V. Ortiz, Q. Cui, A.G. Baboul, S. Clifford, J. Cioslowski, B.B. Stefanov, G. Liu, A. Liashenko, P. Piskorz, I. Komaromi, R.L. Martin, D.J. Fox, T. Keith, A.M.A. Laham, C.Y. Peng, A. Nanayakkara, M. Challacombe, P.M.W. Gill, B. Johnson, W. Chen, M.W. Wong, C. Gonzalez, J.A. Pople, Gaussian 09, Revision D01, Gaussian Inc, Wallingford CT, 2009.

[49] J.P. Perdew, K. Burke, Y. Wang, Generalized gradient approximation for the exchange-correlation hole of a many-electron system, Phys. Rev. B 54 (1996) 16533

[50] A.D. Becke, A new mixing of Hartree-Fock and local density-functional theories, J. Chem. Phys. 98 (1993) 1372-1377.

[51] C. Adamo, V. Barone, Toward reliable density functional methods without adjustable parameters: The PBE0 model, J. Chem. Phys. 110 (1999) 6158-6170.

[52] T. Yanai, D.P. Tew, N.C. Handy, A new hybrid exchange-correlation functional using the Coulomb-attenuating method (CAM-B3LYP), Chem. Phys. Lett. 393 (2004) 51-57.

[53] M. Cossi, V. Barone, *Time-dependent density functional theory for molecules in*

liquid solutions, J. Chem. Phys. 115 (2001) 4708-4717.

[54] P. Ordejón, E. Artacho, J. M. Soler, Self-consistent order-N density-functional calculations for very large systems. Phys Rev B 53 (1996) R10441-R10444.

[55] J. M. Soler, E. Artacho, J. D. Gale, A. García, J. Junquera, P. Ordejón, D. Sánchez-Portal, The SIESTA method for *ab initio* order-*N* materials simulation, J. Phys.: Condens. Matter. 14 (2002) 2745-2779.

[56] D. Sánchez-Portal, P. Ordejón, E. Artacho and J. M. Soler, *Density-functional method for very large systems with LCAO basis sets,* Int. J. Quantum. Chem. 65 (1997) 453-461.

[57] J.P. Perdew, K. Burke, M.Ernzerhof, Generalized gradient approximation made simple, Phys. Rev. Lett. 77 (1996) 3865-3868.

[58] M.J. Lundqvist, M. Nilsing, P. Persson, S. Lunell, DFT study of bare and dye-sensitized TiO_2 clusters and nanocrystals, Int. J. Quantum. Chem. 106 (2006) 3214-3234.

[59] N. M. Óboyle, A. L. Tenderholt and K. M. Langner, cclib: A library for package-independent computational chemistry algorithms, J. Comp. Chem. 29 (2008) 839-845.

[60] J. Preat, D. Jacquemin, E.A. Perpete, Towards new efficient dye-sensitized solar cells, Energ. Environ. Sci. 3 (2010) 891-904.

[61] S. Ardo, G.J. Meyer, Photodriven heterogeneous charge transfer with transition-metal compounds anchored to TiO_2 semiconductor surfaces, Chem. Soc.

Rev. 38 (2009) 115-164.

[62] G.M. Hasselman, D.F. Watson, J.R. Stromberg, D.F. Bocian, D. Holten, J.S. Lindsey, G.J. Meyer, Theoretical solar-to-electrical energy-conversion efficiencies of perylene−porphyrin light-harvesting arrays, J. Phys. Chem. B 110 (2006) 25430-25440.

[63] Y.Jiao, W. Ma, S. Meng, Quinoid conjugated dye designed for efficient sensitizer in dye sensitized solar cells, Chem. Phys. Lett. 586 (2013) 97–99.

[64] W. Ma , Y. Jiao, S.g Meng, Predicting energy conversion efficiency of dye solar cells from first principles, J. Phys. Chem. C 118 (2014) 16447–16457.

[65] J.-Z. Zhang, J. Zhang, H.-B. Li, Y. Wu, H.-L. Xu, M. Zhang, Y. Geng, Z.-M. Su, Modulation on charge recombination and light harvesting toward high-performance benzothiadiazole-based sensitizers in dye-sensitized solar cells: A theoretical investigation, J. Power Sour. 267 (2014) 300-308.

[66] M. J. Lundqvist, M. Nilsing, S. Lunell, B. Akermark, P. Persson, Spacer and anchor effects on the electronic coupling in ruthenium-bis-terpyridine dye-sensitized TiO_2 nanocrystals studied by DFT, J. Phys. Chem. B 110 (2006) 20513-205254.

[67] C. Kormann, D. W. Bahnemann, M. R. Hoffmann, Preparation and characterization of quantum-size titanium dioxide, J. Phys. Chem. 92 (1988) 5196–5201.

[68] R. Sánchez de Armas, J. Oviedo, M.A. San Miguel, J. F. Sanz, Direct vs indirect mechanisms for electron injection in dye-sensitized solar cells, J. Phys. Chem. C

115 (2011) 11293–11301.

[69] D. M. Newns, Self-consistent model of hydrogen chemisorption, Phys. ReV. 178 (1969) 1123.

[70] F. Labat, I. Ciofini, H.P. Hratchian, M. Frisch, K. Raghavachari, C.Adamo, A theoretical investigation of the ground and excited states of selected Ru and Os polypyridyl molecular dyes, J. Am. Chem. Soc. 131 (2009) 14290–14298.

[71] F. Labat, T. Bahers, I. Ciofini, C. Adamo, First-principles modeling of dye-sensitized solar cells: challenges and perspectives, Acc. Chem. Res. 45 (2012) 1268–1277.

Table 1 Computed energy levels and HOMO-LUMO gaps for the DPP-based dyes at B3LYP/6-31G(d,p) level of theory.

	HOMO (eV)	LUMO (eV)	Gap (eV)
DYE-M	-4.93	-2.73	2.20
DPP-T	-4.89	-2.85	2.04
DPP-CO	-5.02	-2.87	2.15
DPP-CA	-5.03	-2.87	2.16
DPP-I	-4.84	-2.83	2.01

Table 2 The calculated dipole-allowed lowest excited state λ_{max} (nm) for the dyes in dichloromethane solution provided by CPCM-TDCAM-B3LYP/6-311+G(2d,2p). The calculated oscillator strength *f* and main excitation configuration are also listed.

Dyes	λ_{max}	*f*	Main configuration
DPP-T	525.17	1.5617	H →L (55%)

			H → L+1 (28%)
DPP-CO	534.40	1.5316	H → L (61%)
			H →L+1 (27%)
DPP-CA	509.37	1.3260	H → L (63%)
			H →L+1 (28%)
DPP-I	536.45	1.6482	H → L (60%)
			H → L+1 (27%)
DYE-M	407.57	1.9728	H-1→ L (69%)
			H→ L (14%)

Figure Captions

Fig.1 Molecular structures of 4 metal-free DPP-based organic dyes with different donors.

Fig.2 Isosurfaces of the selected frontier orbitals at B3LYP/6-31G(d,p) in gas phase for the DPP-based dyes, together with the model dye and the single DPP molecule. The isovalue is 0.02 au.

Fig.3 The calculated absorption spectra for the DPP-based dyes dissolved in dichloromethane at CPCM-TDCAM-B3LYP/6-311+G(d,p)//B3LYP/6-31G(d,p) level of theory.

Fig.4. The calculated LHE curves for the DPP-based dyes.

Fig. 5. The isosurfaces for the HOMO (a), LUMO (b), and the interacting orbial for a

bidentate binding mode of dye DPP-T on the $(TiO_2)_{46}$ nanoparticle. The isovalue is 0.01 au.

Fig. 6. Total DOS (red) and the adsorbate-projected DOS (green) with arbitrary units. Blue and green arrows mark the position of HOMO and LUMO of adsorbed dye molecules.

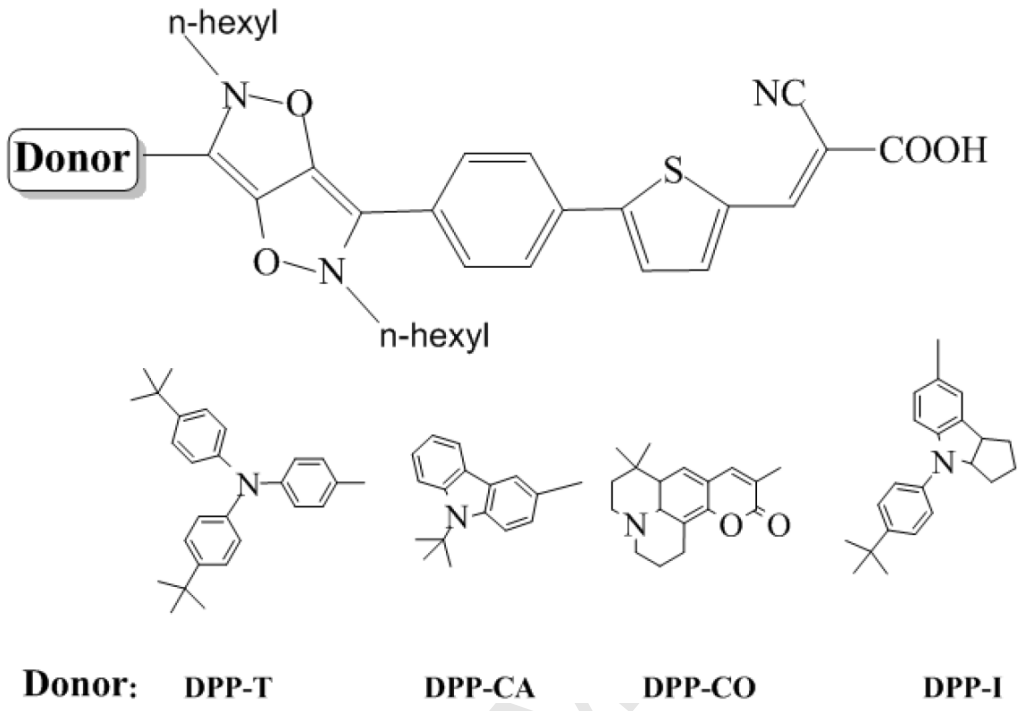

Fig.1

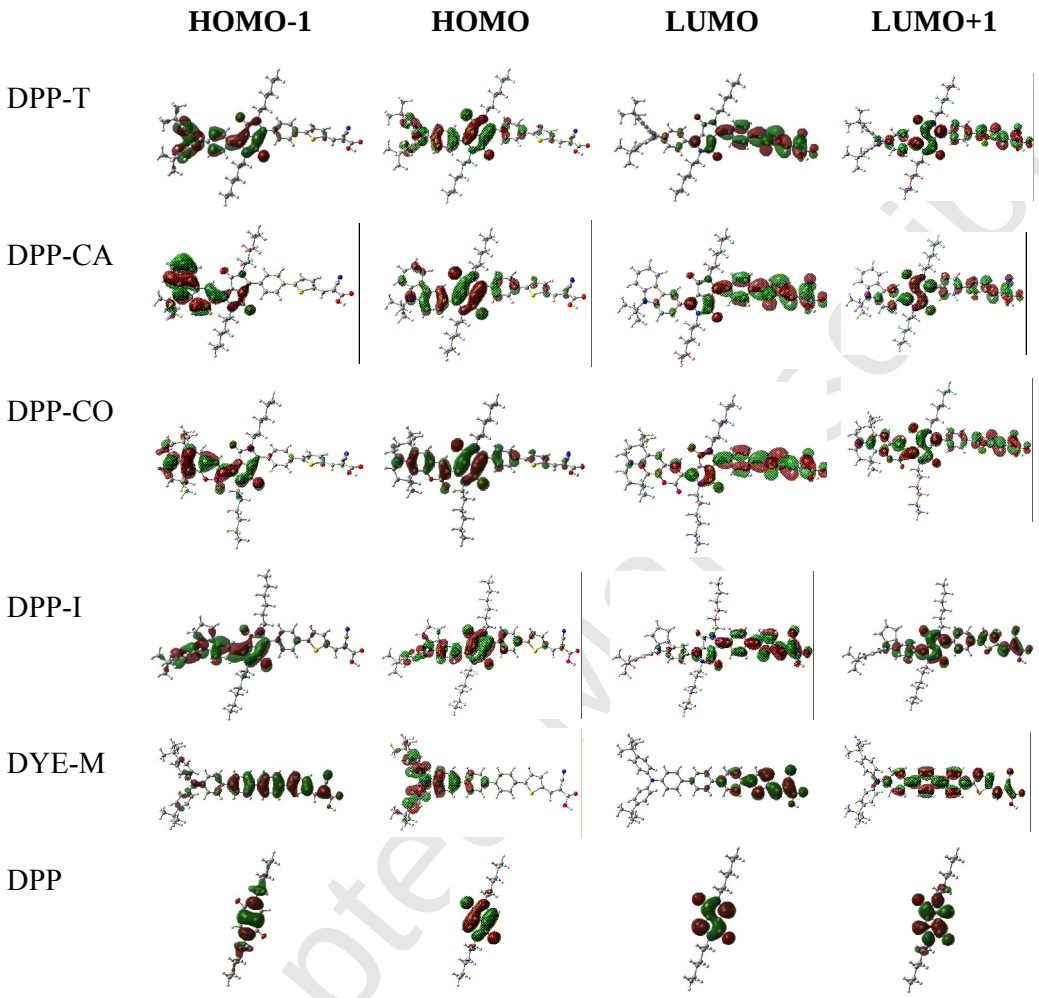

Fig.2

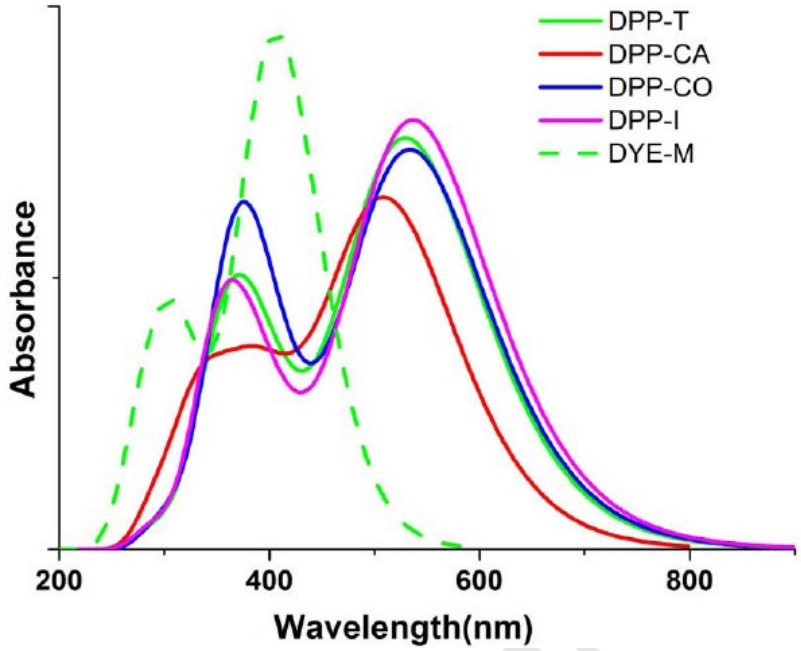

Fig.3

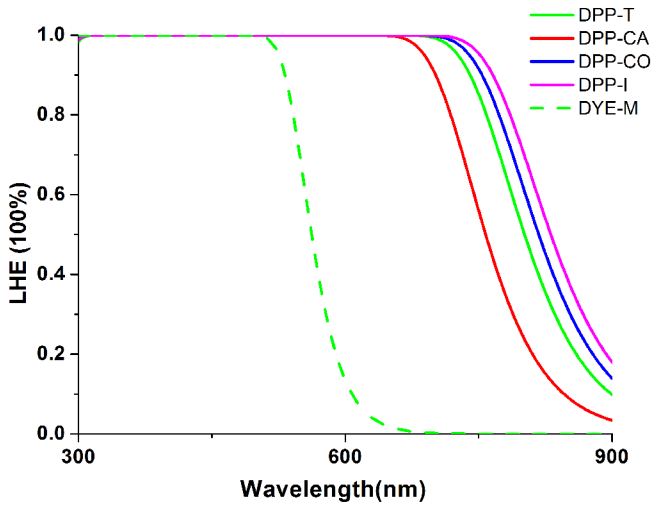

Fig.4

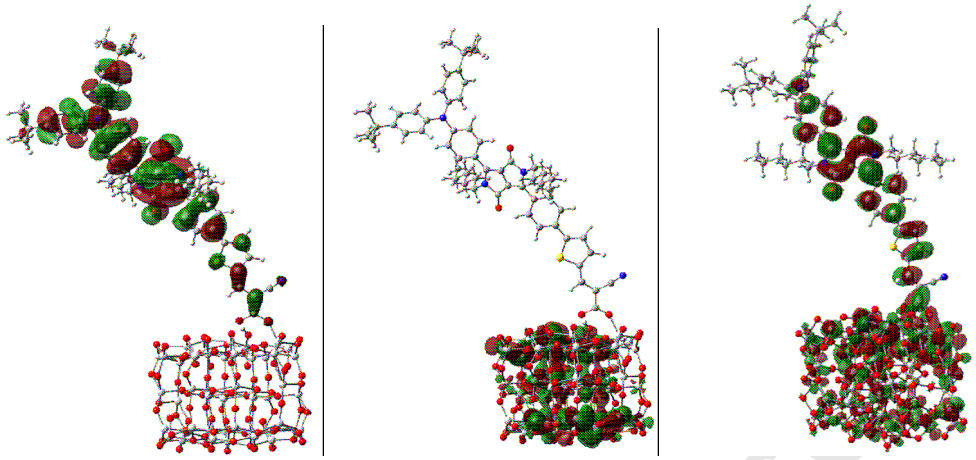

(a) (b) (c)

Fig.5

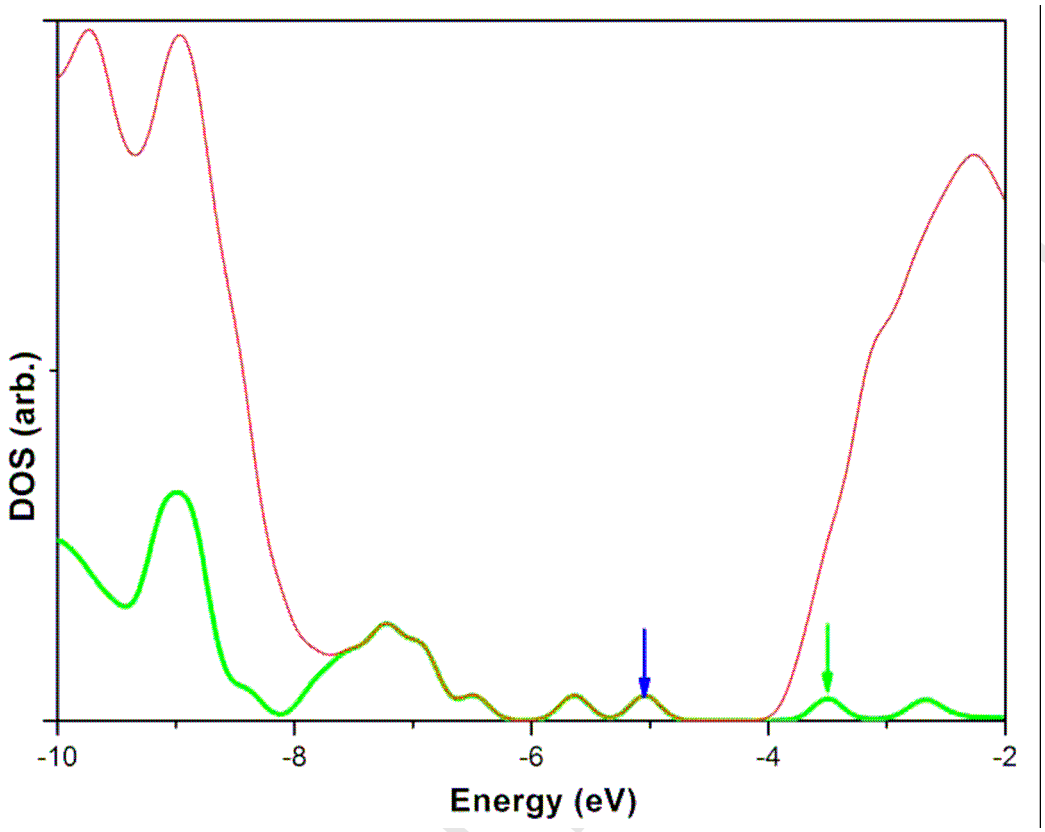

Fig.6